ISSN 1069-3513, Izvestiya, Physics of the Solid Earth, 2016, Vol. 52, No. 4, pp. 503–519. © Pleiades Publishing, Ltd., 2016.
Original Russian Text © A.A. Gusev, E.M. Guseva, 2016, published in Fizika Zemli, 2016, No. 4, pp. 35–51.

Shear Wave Attenuation Estimated from the Spectral Decay Rate in the Vicinity of the Petropavlovsk Station, Kamchatka

A. A. Gusev[a, b] and E. M. Guseva[b]

[a] *Institute of Volcanology and Seismology, Russian Academy of Sciences, bulv. Piip 9, Petropavlovsk-Kamchatskii, 683006 Russia*
e-mail: gusev@emsd.ru

[b] *Kamchatka Branch, United Geophysical Survey, Russian Academy of Sciences, bulv. Piip 9, Petropavlovsk-Kamchatskii, 683006 Russia*
e-mail: emg@emsd.ru

Received September 18, 2014; in final form, May 7, 2015

Abstract—The parameters of *S*-wave attenuation (the total effect of absorption and scattering) near the Petropavlovsk (PET) station in Kamchatka were estimated by means of the spectral method through an original procedure. The spectral method typically analyzes the changes with distance of the shape of spectra of the acceleration records assuming that the acceleration spectrum at the earthquake source is flat. In reality, this assumption is violated: the source acceleration spectra often have a high-frequency cutoff (the source-controlled f_{max}) which limits the spectral working bandwidth. Ignoring this phenomenon not only leads to a broad scatter of the individual estimates but also causes systematic errors in the form of overestimation of losses. In the approach applied in the present study, we primarily estimated the frequency of the mentioned high-frequency cutoff and then constructed the loss estimates only within the frequency range where the source spectrum is approximately flat. The shape of the source spectrum was preliminarily assessed by the approximate loss compensation technique. For this purpose, we used the tentative attenuation estimates which are close to the final ones. The difference in the logarithms of the spectral amplitudes at the edges of the working bandwidth is the input for calculating the attenuation. We used the digital accelerograms from the PET station, with 80 samples per second digitization rate, and based on them, we calculated the averaged spectrum of the *S*-waves as the root mean square along two horizontal components. Our analysis incorporates 384 spectra from the local earthquakes with $M = 4–6.5$ at the hypocentral distances ranging from 80 to 220 km. By applying the nonlinear least-square method, we found the following parameters of the loss model: the *Q*-factor $Q_0 = 156 \pm 33$ at frequency $f = 1$ Hz for the distance interval $r = 0–100$ km; the exponent in the power-law relationship describing the growth of the *Q*-factor with frequency, $\gamma = 0.56 \pm 0.08$; and the loss parameter beneath the station $\kappa_0 = 0.03 \pm 0.005$ s. The actual accuracy of the estimates can probably be somewhat lower than the cited formal accuracy. It is also established (with a confidence level of 10%) that the losses decrease with distance.

DOI: 10.1134/S1069351316030034

INTRODUCTION

The study of seismic wave attenuation with distance provides fundamental information about the inelasticity and scattering properties of the Earth's interior. Knowledge of the attenuation is also required for estimating the source spectra, seismic energy, seismic moments, and other source parameters of the earthquakes, for modeling the probable strong ground motion, etc. The attenuation issues are interesting from the general scientific standpoint; besides, it is also important to know the actual attenuation properties in a particular region. Hereinafter the attenuation is understood as the total energy losses of a wave which are due to both the absorption (inelastic losses) and wide-angle scattering, whereas the amplitude decay due to geometrical spreading is disregarded. The seismic energy scattered into a small-angle cone is considered jointly with the energy of direct waves, which is a common practice in seismology. We avoid using the nomenclature of engineering seismology where the attenuation is understood as the combined effect of the geometrical spreading and losses. At the regional distances and high frequencies (1–50 Hz), the attenuation as a phenomenon has been studied quite poorly. Some fundamental issues such as the relative role of the path (ray) itself, on one hand, and the ground/geological conditions in the vicinity of the receiver (the site effect—contribution of the local features), on the other hand, as well as the character of the frequency dependence of the *Q*-factor, remain poorly known.

There are two common but qualitatively different approaches to studying attenuation. The first (direct) approach considers the gross attenuation—it analyzes the decay of the amplitudes or amplitude spectra with distance. Further, for estimating the losses, some

assumptions are typically made about geometrical spreading. The effect of geometrical spreading on the amplitudes is then eliminated, and the residual is considered as the total effect of the scattering and absorption along the path. The site effect (the contribution of local conditions to the losses) remains unknown. The second (spectral) approach explores the fact that the spectral shape is distance dependent. Here, some assumptions constraining the shape of the amplitude spectra at the source are made, and the change in the shape of the observed spectra is analyzed. If it can be presumed that the waves have an identical type of geometrical spreading across the entire studied frequency band, the particular character of spreading can be set aside. For the case of the sufficiently high frequencies studied below, the waves can be treated as body waves and the geometrical spreading can be assumed to be frequency-independent. The losses determined from the spectral changes are considered as the total effect of the scattering and absorption. The advantages of the direct approach are associated with the fact that the latter enables the attenuation to be studied directly, without any hypotheses regarding the particular source spectrum. However, the necessity to accept the hypothesis concerning the spreading is the weak point of this approach. Besides, some difficulties arise in the estimation of the site effect unless the normalization to the coda wave amplitudes is applied (assuming that the site effect is identical for the direct waves and coda). A strong point of the spectral approach lies in the fact that it provides a possibility to study the attenuation alone, both along the path and in the vicinity of the receiver. However, it is required in this case to hypothesize the spectrum of the source, to assume the smallness of the spectral anomalies at the site, and to consider geometrical spreading as frequency-independent. The last assumption is in some cases vital. This approach is useful for analyzing the data from a single (isolated) station. This is the spectral approach that is applied in the present work.

Both the cited approaches contain an important and scarcely discussed simplification associated with treating the scattering-related losses. Let us consider this simplification for the case of body waves. Typically, it is implicitly assumed in seismology that phases, groups, or wave trains of the body waves can be clearly identified on a seismogram. The case of a local earthquake with a long source duration when the *P*-waves from the late stages of the source process are superimposed on the *S*-wave arrivals is an evident problematic point. We put this case aside and confine ourselves to considering the small and moderate earthquakes when the source duration is not very long. Furthermore, we only consider the important case of *S*-waves. The practice shows that the clear identification of the *S*-group is not always possible even in the case of a small earthquake. Quite frequently, the *S*-group is gradually replaced by coda, and there are no clear indications of its end. This phenomenon is related to wave scattering (or multipath propagation).

In optics and acoustics, scattered waves are understood as the waves propagating from an obstacle (a scatterer) in any direction different from that of incident wave. This definition also includes the waves scattered at low angles. The energy of these waves is considered as totally scattered and is included in the losses. The practice of regional seismology is different: the waves scattered at low angles, which are barely distinguishable in practice from the direct wave, are considered together with the latter. Only the energy of the waves scattered by the wide angles is treated as lost. In particular, the group of *S*-waves is identified by seismologists and considered for convenience as a direct wave, although it is actually formed jointly by the direct waves and the waves scattered at low angles. The energy losses for this group of waves have two components: the losses due to the wide-angle scattering, which is discussed in the present work, and the losses due to the absorption (inelastic losses). The *Q*-factors associated with these two components are denoted by Q_{sc} and Q_i, respectively; the total losses are represented in terms of the total *Q*-factor Q_t or, simply, *Q*; here, $Q_t^{-1} = Q_{sc}^{-1} + Q_i^{-1}$.

Ideally, it is desirable to use the theory of scattered waves for analyzing the observed picture. Such approaches are being developed; they give hope for separately estimating the contributions of scattering and absorption. As a typical example of methods of such kind we cite the Multiple Lapse Time Window Analysis (MLTWA), see, e.g., (Abubakirov, 2005). In this method, the parameters of the envelopes of the actual records after their bandpass filtering are compared to the parameters of the calculated envelopes. The latter are calculated from the model of a homogeneous medium with isotropic scattering and inelastic losses. The comparison of the model to the observed curves enables a separate estimation of the parameters of scattering and inelastic losses. However, the estimates obtained by this method should be treated as tentative. The point is that the models that are used in the MLTWA-based interpretation typically neglect some factors of the real medium such as the evident absence of isotropy in the scattering and a strongly pronounced vertical heterogeneity of the coefficient of scattering. Ignoring these factors can distort the estimates severalfold (Gusev and Abubakirov, 1996; 1999). As of now, the models allowing for these factors have been developed quite poorly. In this situation, using a more primitive approach that separates the *S*-wave groups is the only possibility. The location of the end of the *S*-group is specified to some extent arbitrarily, either interactively or automatically.

Let us review several issues associated with the use of the spectral approach. The spectral approach was initially applied for very simple models of the source spectrum and spectral structure of the losses. It was assumed that (1) the acceleration spectrum in the

source is flat; (2) the losses in the medium are described by a frequency-independent Q-factor; and (3) the Q-factor does not depend on the epicentral or hypocentral distance. In reality, all the three cited hypotheses are inaccurate. Therefore, the model which is used for interpretation in the present work allows each of them to be violated. Let us discuss these points in greater detail.

We start with the source spectrum. In the early works (Gordeev and Rykunov, 1976; Anderson and Hough, 1984), when applying the spectral approach, it was hypothesized that the acceleration source spectrum is flat. This behavior is characteristic of the classical Aki–Brune omega-square model of the source (displacement) spectrum in the frequency band much above the corner frequency f_c. In such cases, the observed acceleration spectrum has an approximately flat segment (plateau), which is limited at the high-frequency side by a clearly expressed upper cutoff. Ideally, the position of this cutoff should be directly related to the integral losses along the ray path. However, as noted by Hanks (1982), the attempt to fully compensate these losses by using the experimental attenuation estimates in the medium is typically ineffective. Hanks designated the frequency of this residual cutoff by $f_{\max}$. Soon after this, Anderson and Hough showed (1984) that the formation of this stable cutoff is probably associated with the significant losses in the upper part of the profile in the immediate vicinity of the station. In their reasoning, they accepted the hypothesis of a constant and frequency-independent Q-factor. In this case, for estimating the attenuation it is sufficient to estimate a single parameter denoted by t^* or κ, which is closely related to $f_{\max}$. The parameter κ is defined by $\kappa = \int_l dr/cQ$, where dr is the ray element, l is the ray path, and c is the wave velocity. In the regional and engineering seismology problems, the path (and, correspondingly, the cited integral) naturally splits into two parts. One part of the path is a very short segment in the upper part of the section directly beneath the station or beneath the construction site. In practice, its contribution to the integral, denoted by κ_0, can be assumed to be constant. For the remaining part of the ray trace, its contribution to the integral grows with distance either linearly or in a more sophisticated way. This contribution is hereinafter denoted by κ_v. Remarkably, in the cited integral we may well assume $\kappa = \kappa(f)$, $Q = Q(f)$. We note straight away that in the interpretation in the present work it will be assumed that κ_0 does not depend on frequency, whereas κ_v is frequency dependent.

As was noted, Anderson and Hough (1984) suggested estimating κ from the decay of the spectrum of a local earthquake with frequency assuming that the acceleration spectrum in the source is flat. This approach has become widespread. A number of subsequent works refined Anderson and Hough's procedure: the records of quakes with sufficiently high f_c were used; the shapes of the source spectra of these quakes were approximated by the Brune model with f_c considered as an additional unknown parameter (Boatwright et al., 1991; Fletcher and Boatwright, 1991). These modifications retain the assumption of a plateau of the acceleration source spectrum at high frequencies. An important element of these works lies in the fact that they use the combined approach where Q is estimated in the course of a single two-step inversion. Here, the information about the losses is inferred from both cited sources: from the decay of spectral amplitudes with distance and from the change in the spectral shape with frequency. With this approach, the joint estimate of Q by the two qualitatively different methods should provide a stable result of the inversion. In this case, geometrical spreading is either assumed to obey the power law (whose exponent is treated as an unknown), or it is calculated beforehand from the given crustal velocity profile.

The fact that the spectrum is specified by the Brune model is a debatable point of this technique. In this model, the formation of $f_{\max}$ is fully attributed to the frequency-dependent losses in the medium. However, there are cases when the high-frequency cutoffs are clearly observed in the acceleration spectra that have been already corrected for the losses both along the path and beneath the site. These facts suggest a partially source-related origin of $f_{\max}$. In other words, the observed $f_{\max}$ can have a complex origin and be formed due to both the frequency-dependent losses during wave propagation in the medium and due to the presence of the upper limit in the source acceleration spectrum. The existence of such a limiting boundary was first hypothesized by (Papageorgiou and Aki, 1983; Gusev, 1983; 1984). This boundary is hereinafter referred to as f_{c3} (Fig. 1). This hypothesis was initially suggested for explaining the formation of $f_{\max}$ by the source effects. However, as was noted above, Anderson and Hough soon demonstrated that a vital role in the formation of $f_{\max}$ is played by the losses beneath the receiver in the immediate vicinity of the station. In these conditions, even in the case of accurate compensation for the attenuation along the main part of the path the HF spectral knee cannot be ascribed to the source alone. The phenomenon of $f_{\max}$ has come to be regarded as related to the losses beneath the station, and the hypothesis of the existence of f_{c3} was, in fact, abandoned by the most seismologists.

Nevertheless, the source-controlled $f_{\max}$ was still clearly identified in a number of cases (Kinoshita, 1992; Gusev et al., 1997; Sasatani, 1997); a brief review can be found in (Gusev, 2013). Presently, the existence of the source contribution to the $f_{\max}$ phenomenon is typically admitted in principle (Purvance and Anderson, 2003); however, the question still needs thorough investigation. The key difficulty in identifying $f_{\max}$ lies in the fact that the observed $f_{\max}$ reflects the response of the white-noise acceleration signal to the

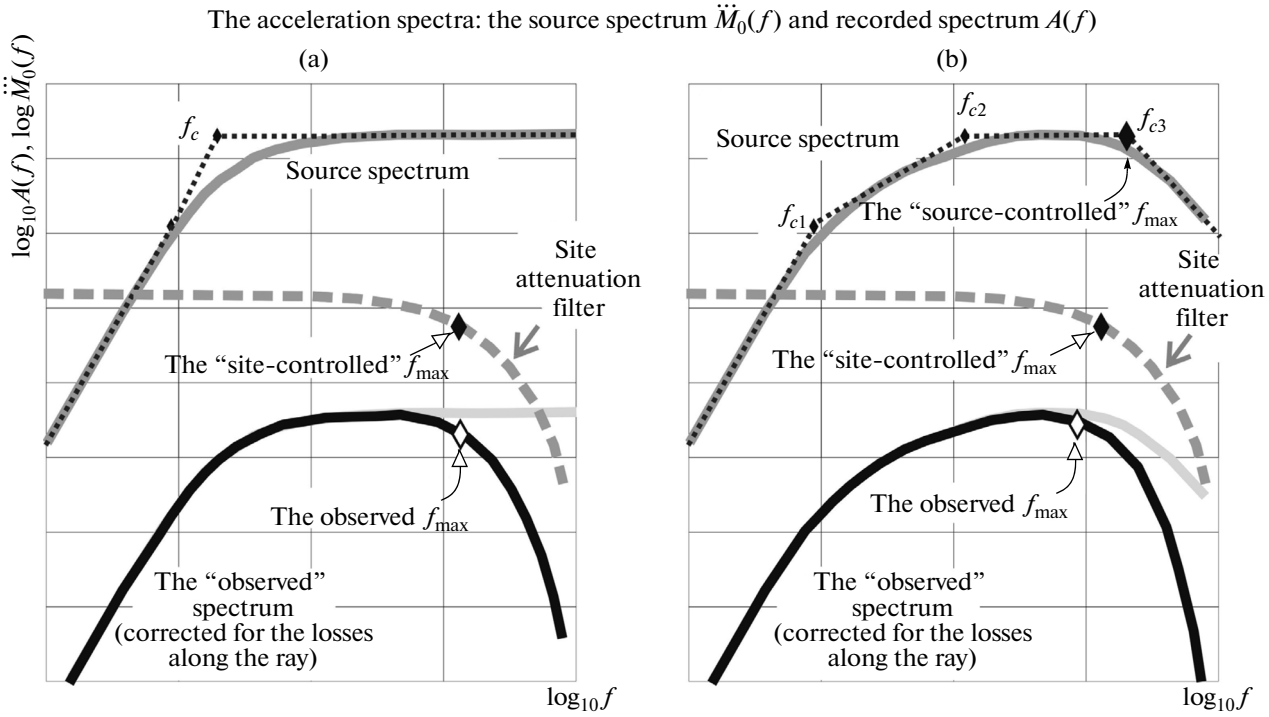

Fig. 1. The schematic (Fourier) amplitude spectrum of the body-wave acceleration. The top curves show the source acceleration spectrum (SAS or $\ddot{\dot{M}}_0(f)$,; the bottom curves show the corrected site spectrum $A(f)$ (the observed spectrum in which all the losses but those related with the ground layer immediately beneath the station are compensated). The middle dashed line depicts the transfer function of the absorption operator in the soil layer, whose action forms (partially or fully) the upper cutoff, f_{max}, of the recorded acceleration spectrum. (a) The case of the standard Brune SAS model with a single corner frequency f_c. In this case, the value of f_{max} is fully determined by the medium. We denote it by $f_{max}^{(m)}$. Typically, the model works reasonably well in the case of the small earthquakes; however, it is also frequently applied for the strong seismic events (with magnitudes $M = 6$ and higher). (b) The similar spectra for the SAS model used in the present work, with three corner frequencies f_{c1}, f_{c2}, and f_{c3}. The model is suitable for describing the spectra of the earthquakes with any magnitudes. In case (a), f_{c1} and f_{c2} coincide; and if the spectral corners at f_{c1} and f_{c2} are clearly discernible in the observed spectra, it is traditionally a common practice to assume the Brune spectral model with $f_c = (f_{c1}f_{c2})^{0.5}$. The frequency value f_{c3} here plays the role of the source-controlled f_{max}, or $f_{max}^{(s)}$. The combination of two cutoffs, $f_{max}^{(m)}$ and $f_{max}^{(s)}$, results in the emergence of the observed "joint" upper cutoff f_{max}. The following relationships are always valid: $f_{max} < f_{max}^{(m)}$ and $f_{max} < f_{max}^{(s)}$. Frequently (particularly for the small earthquakes), $f_{max}^{(m)} \ll f_{max}^{(s)}$; then, the observed f_{max} (typically 5–15 Hz in such cases) is determined by the losses beneath the station and it gives the estimate for $f_{max}^{(m)}$. In same cases, also the opposite relationship is valid in some cases, particularly for the strong earthquakes: $f_{max}^{(s)} \ll f_{max}^{(m)}$, and then the observed f_{max} (typically of the order of 2–4 Hz) is determined by the source and gives the estimate for $f_{max}^{(s)}$.

simultaneous action of two filters with the commensurate cutoff frequencies (Fig. 1). The possibility that such a combination can in principle exist was noted as early as 1984 (Anderson and Hough, 1984, Fig. 13 therein); however, the ways for the interpretation of the spectra in such a case were not discussed.

In this situation, a vicious circle appears: in order to estimate f_{c3}, one should compensate the loss effects; however, it is unclear how could the losses be evaluated independently, without a priori knowledge of f_{c3}. Attempts were made to use the model in which the source- and path-related contributions to the observed value of κ are additive (Purvance and Anderson, 2003) or multiplicative (Tsai and Chen, 2000); however, the results did not provide a clear solution. In order to eliminate the influence of the losses beneath the station (together with the distorting effects of the transfer function of the soil layer beneath the station), Sasatani (1997) and Gusev (2013) calculated the ratio between the spectra from two earthquakes recorded by the same station. In this case, the calculations give an estimate of f_{c3}; however, this can only be done in the special cases when f_{c3} significantly differs between the components of a pair of the earthquakes. This approach is inapplicable for systematic study. At the same time, without separating the effects associated with the

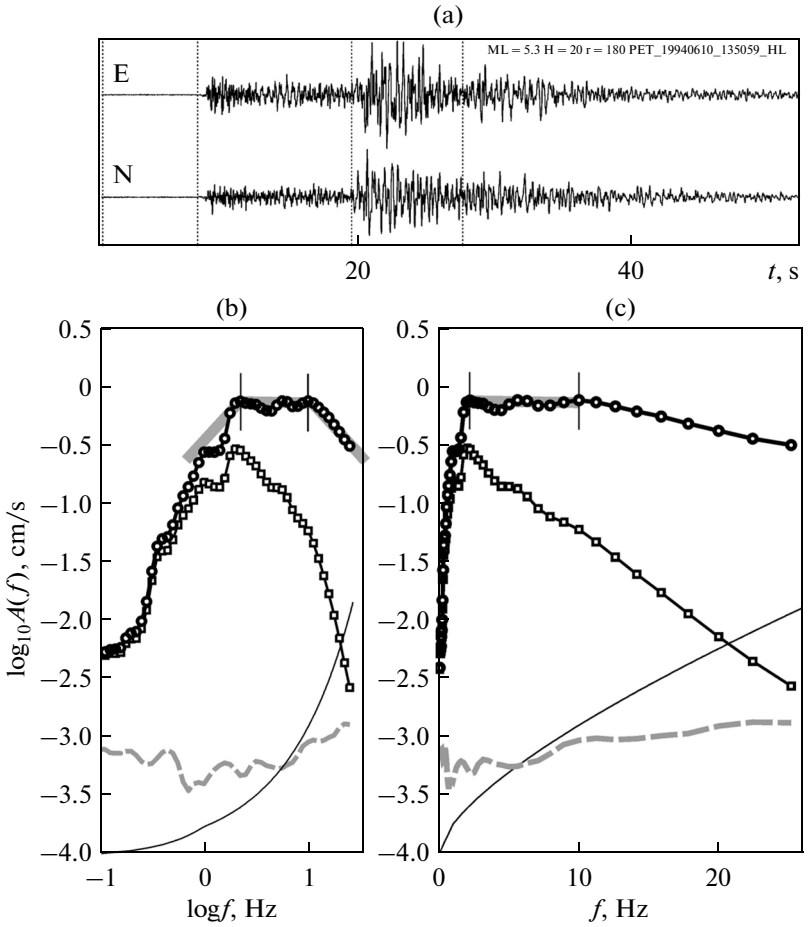

Fig. 2. The example of processing the records of the *S*-waves from the earthquake of June 10, 1994, 13:25, $M_L = 5.3$, $H = 20$ km; $r = 180$ km. (a) The initial records of the horizontal acceleration components (the vertical scale is arbitrary). Two pairs of the dashed lines mark the interval of calculating the amplitude spectra of the noise and *S*-waves; (b) the observed spectrum $A(f)$ (squares), the spectrum corrected for absorption $A_1(f)$ (circles), and the noise spectrum (the gray dashed line), all reduced to $r = 1$ km. The thin line in the bottom part of the plot is the operator of loss correction by the model 2013, which was used in the present analysis (see Table 1). This line is shifted downwards for better visualization. The gray broken line approximates the plateau and its vicinity in the corrected spectrum. The approximation of the plateau in the acceleration spectrum, which was used for the further processing, is shown by the vertical segments; they correspond to the frequencies f_{c2} and f_{c3}. The scale is log-log. (c) The same, on the semi-log scale. It can be seen that the presence of the corner point at f_{c3} in the semi-log graph of the non-corrected spectrum is almost unnoticeable. All log scales are in $\log_{10}$ units.

source and the medium, it is in principle impossible to isolate and accurately estimate the contribution of one factor (the losses along the path). In the present work, we try to find the approaches to solving this problem.

Another debatable point mentioned above lies in the assumption of a frequency-independent Q, which is used in some studies. In the reality, this assumption is violated for both the mantle overall (Lekić et al., 2009) and for the lithosphere. The estimates of Q by the direct method systematically testify to the presence of this dependence (Fedotov and Boldyrev, 1969). The same conclusion also ensues from the spectral method. For example, Trifunac (1994) analyzed the acceleration spectra from the earthquakes in the western United States and revealed a clearly pronounced frequency dependence of the losses. This dependence is also demonstrated in the special study of Ford et al. (2008), who compared five technologies for estimating Q. We also cite the paper (Malagnini et al., 2007) where, based on the extensive and reliable data for California, the authors obtained a model with a distinct frequency-dependent Q close to $Q = 180f^{0.42}$. The discussion of the frequency dependence of Q is still ongoing.

After all, there is also a problem concerning the dependence of the estimates of κ and Q on the hypocentral distance. For example, Hough et al. (1988) and Trifunac (1994) reported a prominent dependence of this kind for California: the losses (Q^{-1}) decrease with distance. This trend is probably due to the fact that the rays penetrate deeper into the Earth's interior as distance increases, whereas the losses (Q^{-1}) decrease with depth. It is likely that this phenomenon is almost ubiquitous. For example, Castro et al. (2008) not only

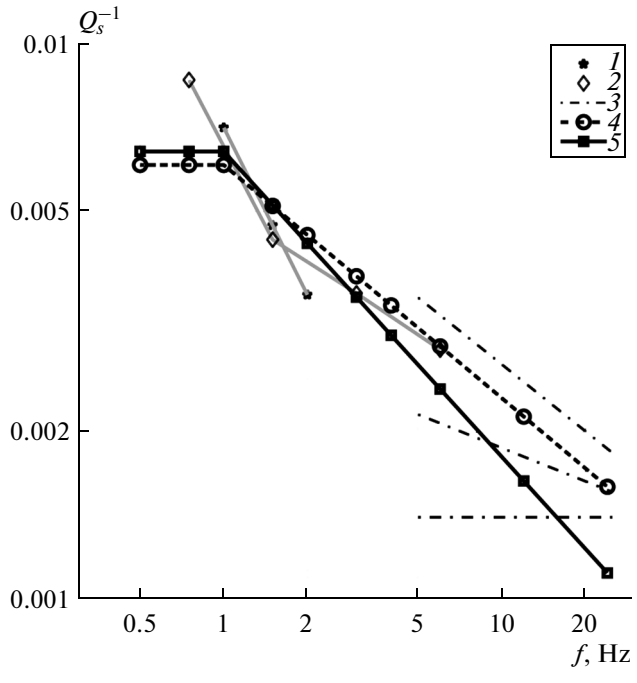

Fig. 3. The forms of frequency dependences of Q^{-1} for $r = 100$ km: *1*, according to (Gusev and Shumilina, 1999), a point estimate with fuzzy binding to frequency; *2*, according to (Abubakirov, 2005), direct empirical estimate; *3*, three patterns of $Q^{-1}(f)$ dependence obtained based on the estimate of κ from (Gusev and Guseva, 2012) for the interval 5–25 Hz, with the three fixed assumed values of $\gamma = 0$, 0.2, and 0.4 (from bottom to top); *4*, the estimate from (Gusev and Guseva, 2013) used for spectral correction; *5*, the result of the present analysis.

established the presence of this dependence for Northern Italy but also interpreted it in the context of the two-layer model of the crust and upper mantle. According to this model, Q^{-1} in the upper layer is more than tenfold larger than in the lower layer (at $f = 2$–3 Hz). A quite significant loss reduction with distance is revealed by Kurtulmus and Akyol (2013) in Western Turkey. Thus, a single parameter of the medium Q^{-1} that neither depends on frequency nor on distance is insufficient for accurately characterizing the losses. The cited relationships should be studied directly.

The present work is primarily intended for studying the *S*-wave attenuation on a new methodical basis with a joint allowance for all the critical points noted above: the complex nature of f_{max}, the frequency dependence of Q, and the dependence of Q on distance. For separating the contributions of the source and the propagation medium into the high-frequency decay of the acceleration spectrum (the f_{max} phenomenon), we use a two-step approach. Initially, the observed spectra are corrected based on the a priori loss estimates (both along the path and beneath the site), and f_{c3} is estimated from the corrected spectrum. Then, the attenuation estimate is refined using as input data of inversion the selected segment of the source spectrum, which is presumably flat. It turned out that the obtained attenuation estimate insignificantly differs from the initial estimate, and therefore the procedure of estimating the attenuation was limited to a single iteration without subsequent refinement.

As the initial observational data, we use the records of the local earthquakes by the Petropavlovsk station, Kamchatka, in the frequency band of 1–30 Hz at the hypocentral distances of 80–220 km. To date, certain knowledge has been obtained about the attenuation parameters for East Kamchatka; a brief review of the earlier works and the latest estimates are presented in (Abubakirov, 2005). MLTWA was the main method used in the cited work. In parallel with this, the estimates were also obtained in a more traditional way—based on the known method of normalizing the amplitude spectra by the coda-wave amplitudes and assuming the $1/r$ geometrical spreading. These estimates can be compared to their independent counterparts obtained in the present work by the spectral method. If this comparison yields consistent estimates, this would enhance the confidence of the results obtained in both works.

The paper has the following organization. We start by discussing the methodical questions and processing algorithms, as well as describing the initial data and initial estimates of the attenuation. Then we present the examples of the data and discuss important practical issues associated with the application of the method, including the selection of the segments in the observed spectra which are suitable for estimating Q. After this, we determine the parameters of the attenuation model assuming frequency- and distance-dependent Q. Both dependences turned out to be pronounced quite distinctly.

THE METHOD AND ITS JUSTIFICATION. THE PROCESSING PROCEDURES

Let A_0 and A be the amplitudes of the sine seismic wave S at the receiver in the absence or presence of attenuation, respectively. The relative losses on path r in a uniformly absorbing medium with quality factor Q can be represented in the following form:

$$A/A_0 = \exp(-\pi f r/cQ) = \exp(-\pi f t/Q) = \exp(-\pi f \kappa), \quad (1)$$

where f is the wave frequency, while c and t are the velocity and travel time of the *S*-wave; and $\kappa = t/Q$ is the parameter of integral losses on the path. In the data analysis, instead of the amplitude of the sinusoidal wave, the estimate of the Fourier amplitude spectrum of the *S*-wave train obtained by averaging the power in a sufficiently narrow frequency band is used. In the analysis in terms of parameter κ, it is often assumed that Q is frequency-independent, which entails the frequency independence of κ as well. Although this assumption is typically oversimplified compared to the real situation, the engineering seismology where the

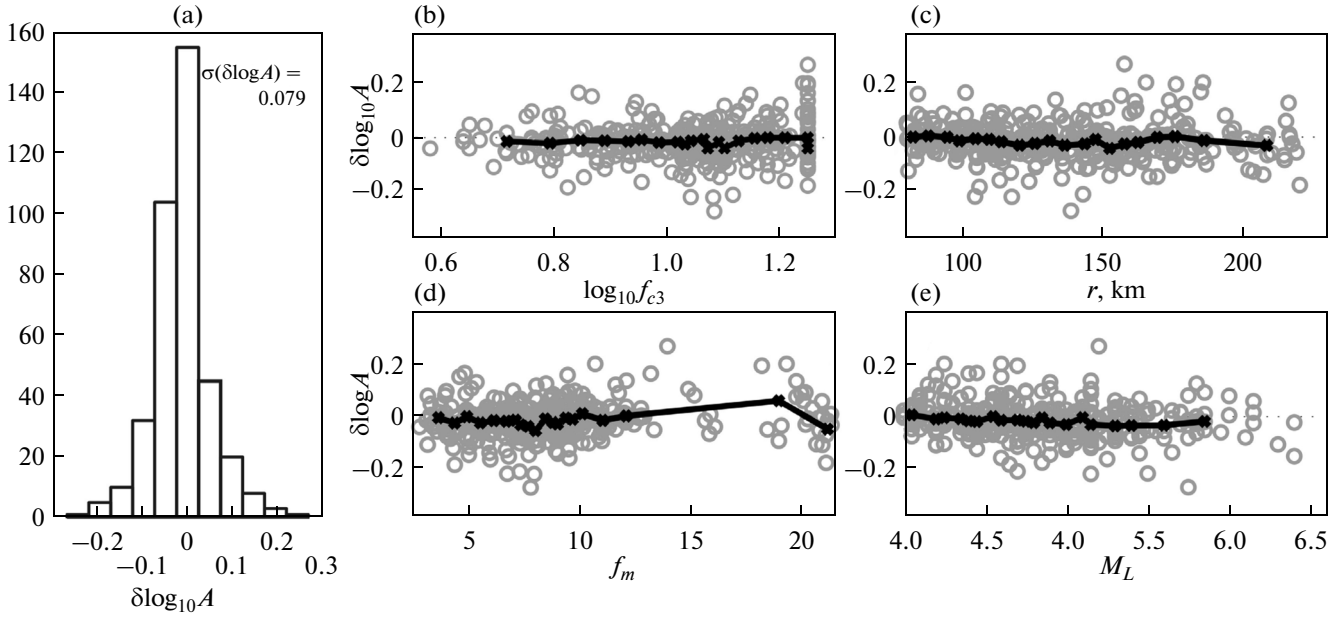

Fig. 4. The errors $\delta\log_{10}A$ of approximation of the observed differences of log amplitudes by the fitted combination of the parameters κ_0, Q_0, γ, and q: (a) the histogram of $\delta\log_{10}A$; also the estimated standard deviation is presented; (b), $\delta\log_{10}A$ as a function of the upper cutoff frequency of the operating bandwidth; (c), $\delta\log_{10}A$ as a function of hypocentral distance r; (d), $\delta\log_{10}A$ as a function of the central frequency f_m of the operating bandwidth; (f), $\delta\log_{10}A$ as a function of M_L. From (a) it can be seen that the distribution is heavy tailed (excess = 5.7) which apparently indicates the presence of a mixture of distributions with different σ. The σ value itself is rather small and it corresponds to the residual scatter of the amplitude of less than 10%. From graphs (b)–(e) it can be seen that the errors are not systematic relative to the studied parameters.

analysis is most frequently based on the parameter κ traditionally assumes a frequency-independent κ, and this is fairly well justified when applied to the component κ_0, as discussed below. We note that for both the teleseismic *P*-waves at ~1 Hz and below and for the surface waves, the hypothesis of frequency-independent Q (and t^*) which is applied quite often should be treated as an oversimplification (Lekić et al., 2009).

At the higher frequencies, the frequency dependence of t^* is fairly distinct even at the teleseismic distances (e.g., see (Venkataraman et al., 2002)) and is clearly pronounced on the local paths. However, at the shortest distances (the site effect or the effect of the uppermost part of the section beneath the station), the losses in the uppermost portion of the profile up to a depth of a few dozen to hundreds of meters beneath the seismic station again quite well agree with the hypothesis of a frequency-independent Q. The contribution of the upper portion of the section in the losses is denoted by κ_0, and the part of the losses that depends on distance and, presumably, on frequency is denoted by κ_v. Importantly, the value of Q in the upper part of the section is much lower than within the main part of the ray path. In the Brune spectral model, it is κ_0 that determines the observed cutoff frequency $f_{\max}$ in the records obtained at a minimal distance from the source. In these cases, κ_0 is roughly $0.2/f_{\max}$. The assumption of a frequency-dependent κ or Q complicates the analysis. However, this is not the last difficulty: the estimates of Q also depend on distance. The probable causes of this dependence are discussed in the Introduction. Thus, the attenuation studies should take into account the frequency and distance factors, as well as allow for the site effect. The latter can be done under the assumption of constant Q.

Considering the described facts, we used the following attenuation model for analyzing the data:

$$-\log\left(\frac{A(f)}{A_0(f)}\right) = \pi f \kappa = \pi f(\kappa_0 + \kappa_v) = \pi f \kappa_0 + \frac{\pi f r}{cQ(f,r)}, \quad (2)$$

where $A(f)$ and $A_0(f)$ are the smoothed amplitude spectra of the *S*-waves near frequency f in the presence or absence of losses, respectively. The loss parameter Q^{-1} is assumed to depend on frequency by the power law (Fedotov and Boldyrev, 1969) and to linearly depend on distance:

$$Q^{-1}(f,r) = Q_0^{-1}\left(\frac{f}{f_0}\right)^{-\gamma}\left(1 + \frac{q(r-r_0)}{r_0}\right), \quad (3)$$

where the parameters Q_0, γ, and q are not known and, together with κ_0, are to be determined from the observations. By using the integral parameter κ_0, we avoid the necessity of specifying the details of the vertical distribution of Q directly beneath the station, which is difficult to do and is typically insignificant for the

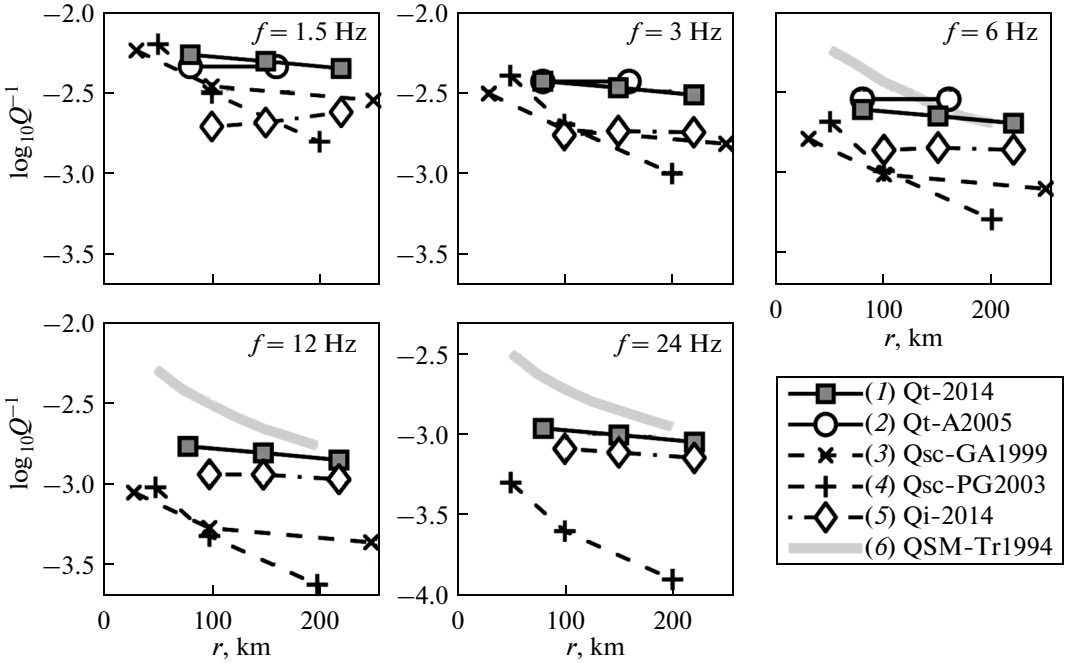

Fig. 5. The dependence on distance for the total losses Q_t^{-1}, the losses due to scattering Q_{sc}^{-1}, and inelastic losses Q_i^{-1} for the medium in the vicinity of the PET station in the five frequency bands (the central frequencies are indicated in the right upper corner of each graph): *1*, the estimates of Q_t, this work; *2*, Q_t according to (Abubakirov, 2005); *3*, Q_{sc} according to (Gusev and Abubakirov, 2003); *4*, Q_{sc} according to (Petukhin and Gusev, 2003); *5*, Q_i, see Table 2; *6*, Q_t according to (Trifunac, 1994) for the west U.S. The increase of the losses Q_i^{-1} with distance at 1.5 Hz is unreliable. Ordinates are in $\log_{10}$ units.

applications. The reference distance r_0 corresponding to the sought Q_0-value is hereinafter assumed to be $r_0 = 100$ km. This value is selected to fall in the working interval of our data which covers a limited range of distances 80–220 km. By substituting (3) into (2), we see that κ_v is, thus, assumed to quadratically depend on distance. The model of a frequency-independent κ, which is quite common, corresponds to the assumption $\gamma = 0$. We assumed $f_0 = 1$ Hz.

For applying the spectral approach, it was necessary to specify a segment on the obtained acceleration spectra within which the source spectrum could be assumed to be flat. This is a challenging problem. The radiation from the source is determined through the source spectrum of the earthquake or through the amplitude spectrum $|\dot{M}_0(f)|$ of th source seismic moment rate $\dot{M}_0(t)$ (the source displacement spectrum (SDS)). The modulus sign $|\cdot|$ is hereinafter omitted. In the most of the works studying the attenuation within the spectral method, it is assumed that $\dot{M}_0(f)$ follows the Brune model (Brune, 1970):

$$\dot{M}_0(f) = \frac{M_0}{1 + (f/f_c)^2}, \qquad (4)$$

where f_c is the corner frequency (the upper cutoff frequency of SDS) and M_0 is the scalar seismic moment. The latter is strictly tied to the moment magnitude determined by

$$M_w = 2/3(\log_{10} M_0\,[\text{dyne cm}] - 10.7). \qquad (5)$$

The local magnitude M_L of the Kamchatka regional network is commensurate with M_w. The far-field ground motion acceleration spectrum is proportional to $\ddot{M}(f)$ (the spectrum of the third derivative of $M_0(t)$). In the case of (4), this spectrum can be cast in the form

$$A_0(f) \sim \ddot{M}(f) = \frac{(2\pi f)^2 M_0}{1 + (f/f_c)^2}. \qquad (6)$$

Function $\ddot{M}(f)$ is referred to as the source acceleration spectrum (SAS). At $f \gg f_c$, assuming that (6) is valid, the dependence of $A_0(f)$ on f is negligible and, therefore, considering (2), we can write out for the observed spectrum $A(f)$ in this interval as

$$\log A(f) = A_0(f) - \pi f \kappa \approx \text{const} - \pi f \kappa. \qquad (7)$$

It may appear that κ can now be estimated as $-\frac{1}{\pi}\frac{d \log A(f)}{df}$, and each spectrum may provide an individual estimate of κ (Anderson and Hough, 1984).

However, the model of the source spectrum (6) is oversimplified and often in contradiction of the observations. Therefore, the direct application of this model for the data analysis may lead to biased estimates. The

question of whether the plateau in the source acceleration spectrum has a source-controlled upper cutoff at f_{c3} is discussed in the Introduction. However, the complications do not end there. As early as in (Brune, 1970), it was noted that the cited main band of the spectrum (at $f = f_c$) may split into two corners at appropriate frequencies (hereinafter denoted by f_{c1} and f_{c2}), between which there is a segment of the source displacement spectrum with the intermediate trend close to f^{-1} or, for the acceleration, a segment of the source acceleration spectrum with the intermediate trend close to f^1 (see Fig. 1). This question was discussed in (Gusev, 1983; 1984); a brief review is presented in (Gusev, 2013). The corner frequency f_{c2}, which is significantly higher than f_{c1}, is discernible in most of the spectra studied in the present work (see (Gusev and Guseva, 2013)). Thus, the lower boundary of the working frequency band should be selected based on f_{c2}, which is noticeably higher than f_{c1}. In the present work, we used the following two-stage algorithm for estimating f_{c2} and f_{c3}: (1) firstly, we considered the preliminary, initial loss estimate which was derived in advance and, based on this estimate, corrected the spectrum by compensating the main part of the losses; (2) secondly, using the obtained estimate of the shape of the source spectrum, we localized f_{c2} and f_{c3} and, thus, determined the frequency band where the true source acceleration spectrum presumably behaves as f^0. After having identified the working frequency range for a given observed spectrum, one can then use the spectral trend within this segment for calculating the attenuation estimates by formula (7) and, thus, obtain a new refined estimate of the losses. This is what was done in the present work.

The first two steps of the described procedure are illustrated by Fig. 2. Based on the acceleration spectra $A(f)$ obtained from the observations, we calculated their modification $A_1(f)$ corrected for losses, which approximately reflects the source acceleration spectrum; the exact correction would yield $A_0(f)$. The $A_1(f)$ curve was approximated by the model of the piecewise–power-law trend. The spectral shape approximation that is close to optimal is fitted interactively; it enables the corner frequencies of the spectrum to be estimated. This approach requires that the frequency interval $[f_{c2}; f_{c3}]$ is sufficiently wide for obtaining the estimate $\kappa = -\frac{1}{\pi}\frac{d \log A(f)}{df}$ from (7). This condition is quite often satisfied.

The described approach is underlain by a number of implicit assumptions which deserve separate discussion. Let us assume that the right-hand side of (2) contains one more term describing the losses which depend on distance but not on frequency. If the analysis is conducted in terms of the components of κ, the mentioned assumption means that there is a term κ' that behaves as $\kappa' \sim 1/f$. This case is not speculative. Firstly, the inaccurately estimated geometrical spreading may always introduce a fictitious contribution of this type into the attenuation estimates. However, the spectral approach applied in this work does not depend on the geometrical spreading and is therefore tolerant to such distortions. Secondly, as hypothesized by Dainty (1981), the contribution of scattering in the losses can be described through $Q_{sc} = Q_{0sc} f^{-\gamma}$ with $\gamma = 1$; this behavior would also introduce the $1/f$-like contribution to κ. The intangibility of these effects is a potential pitfall of the spectral method. However, the contribution of the component with the $1/f$ behavior is actually barely significant because this component should strikingly manifest itself at low frequencies, where the estimates by spectral method can be reliably verified by those provided by the direct method, and such distortions, if strong, can be detected. Another problem of the spectral method lies in the fact that the f^0-type behavior of the source acceleration spectrum is, in fact, an assumption. Of course, the model of a flat source's acceleration spectrum demonstrated its efficiency in many cases; however, this model has never been verified rigorously, and such a verification would be challenging. There are observations suggesting a violation of this model. For example, in their recent accurate study, Ye et al. (2013) obtained quite a reliable estimate of the acceleration spectra for some sources which behave as $f^{0.2-0.4}$ instead of f^0 although,

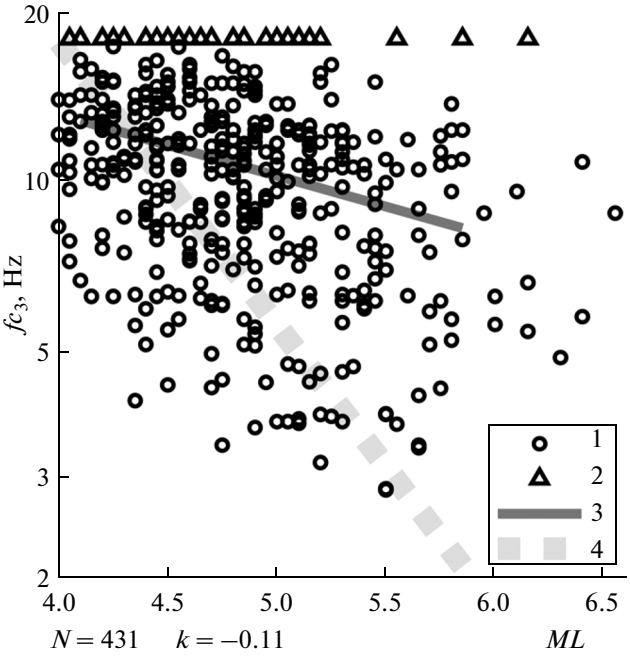

Fig. 6. The dependence of the estimates of f_{c3} on the local magnitude ML: 1, the conventional estimate; 2, the estimate in the form of the inequality $f_{c3} > 18$ Hz; 3, the empirical linear trend $f_{c3}(ML)$) estimated with the combined use of the common data and the data in the form of inequalities; its slope is -0.11 ± 0.017; 4, the same hypothetical trend assuming that the sources are kinematically similar.

remarkably, the case of f^0 proved to be typical. Hereinafter we neglect this problem; however, its reality should be born in mind.

Finally, significant distortions in the case of the spectral approach can arise due to the spectral peculiarities of the station, i.e., due to the differences of the transfer function of the upper part of the profile beneath the receiver from that for the half-space. This factor is difficult to control. The PET station is installed on the intrusive hard rocks where the *P*-wave velocities are about 2.7 km/s. In dozens of studies on the seismic microzoning of the sites close to Petropavlovsk–Kamchatskii based on the spectral ratio of the *S*-waves or coda waves, PET has been always successfully used as the reference hard-rock station and never demonstrated any significant resonant peaks or other peculiarities. Although these considerations are not fully convincing, hereinafter, we assume that the local spectral peculiarities of the PET station are negligible.

INITIAL DATA AND FIRST STAGE OF PROCESSING

The broadband PET (Petropavlovsk–Kamchatskii) seismic station of the IRIS network started operating in Kamchatka in 1993. The records by this station were used as the basis of the present analysis. The use of these data enabled the attenuation in Eastern Kamchatka to be studied in sufficient detail for the first time. The initial data for fitting model (3) were obtained in the following way. We considered all the records by the PET station from the earthquakes that occurred during 1993–2005 at the epicentral distances of r = 80–220 km (the closer earthquakes are extremely rare here) and had magnitudes $M_L = 4$–6.5 ($K^{F68} = 9.5$–14). No depth selection was made. The records with a sampling frequency of 80 Hz are obtained by the FBA-23 accelerometer—Quanterra logger digital channel. After introducing the instrument corrections, we viewed the records and identified the segments of the *S*-waves and the noise before the *P*-wave arrivals. Two techniques were used to identify the segments of the *S*-wave. In the formal technique, the length of the data segment was defined as a fixed fraction x of the *S*-wave travel time, namely, $x = 0.25$. In this case, in the single scattering model, the elementary geometry shows that the typical angles of the scattered rays' deviation from the initial direction are up to 37°. In the case of multiple scattering, the typical deviations are smaller. Therefore, $x = 0.25$ appears to be a reasonable selection. With this approach, a certain part of the signal energy is in some cases rejected. In the second technique, the segment was selected interactively, and the length of the wave group was visually evaluated in such a way that the main fraction of the energy fell in this segment. In this case, the value of x was within 0.10–0.35. A comparison showed that the selection of the processing procedure does not affect the spectral estimates. Hereinafter, we use the results of the second (visual) procedure.

The signal within the segment was subjected to 5% tapering. Then, the amplitude Fourier spectra of the acceleration were calculated by the Fast Fourier Transform (FFT). The amplitude spectra were smoothed by the procedure (Guseva et al., 1989) with a constant logarithmic step in frequency (0.05 of the common logarithm, or 6 points of the output spectrum per octave). The smoothing window had a width of 0.15 of the common logarithm (half an octave). In fact, the smoothing procedure is applied to the squared amplitudes; therefore, the energy of the signal is only subjected to the minimal distortions. After this, the noise spectrum was reduced to the case of a segment of similar duration by multiplying by $(d_s/d_n)^{0.5}$, where d_s and d_n are the durations of the signal and noise segments, respectively. The value of d_n was slightly larger than or commensurate with d_s. The signal and noise spectra for the *S*-waves were determined as the root mean square value of two horizontal components. Next, the noise effects were roughly compensated by subtracting the noise energy from the signal energy. The upper boundary of the operating spectral bandwidth was specified by the condition that the signal-to-noise power ratio is at least 3. The lower boundary of the bandwidth was determined by the requirement that at least two points of the FFT spectrum fall in the averaging band. However, the lower boundary was typically higher than this threshold and was determined by a fairly common burst in the amplitude of the observed displacement spectrum within a range of 0.2–0.3 Hz. This burst is caused by the additional contribution of the high-frequency surface waves into the signal and it should be excluded from the analysis when it is desired to consider the observed signal as a group of the body (*S*) waves. As a result, we obtained the smoothed spectrum of the observed *S*-wave.

For introducing the correction for absorption, we used the tentative estimates $Q(f)$ obtained in the following way. By analyzing the limited data (dozens of records) with sufficiently high amplitudes in the spectral window of 5–25 Hz, we have previously obtained the estimate of κ in this window (Gusev and Guseva, 2012). For this, based on (7), we conducted the linear regression of $\log A(f)$ in f and obtained an estimate of κ as the regression coefficient. The requirement that sufficiently high amplitudes exceeding the noise are present in this window automatically rejected most of the spectra with low f_{c3}. Besides, the visual control sorted out the cases when the dependence $\log A(f)$ was obviously nonlinear. It can be therefore assumed that the fictitious contribution to the absorption due to the bending of the source spectra can only introduce limited distortions to the results. The growth of κ with distance r in a number of the works is approximated by a linear function. In our case, the dependence $\kappa(r)$, against a wide scatter, demonstrated a clear deceleration of the growth rate of κ with distance. The follow-

ing, rather coarse estimates were obtained: $\kappa = 0.053$ s (0.070 s) for $r = 100$ km (200 km, respectively). Here, the κ value in brackets corresponds to the second value of the distance. Below, we keep to this convention. The estimate of κ_0 has a low accuracy. It is assumed to be 0.016 s, which yields the estimates $\kappa_v = (r/c)Q^{-1}(f,r)$, for $\kappa_v = \kappa - \kappa_0 = 0.037(0.054)$ (see formulas (2) and (3)). Under the hypothesis of a frequency-independent Q, the Q estimate for the frequency band of 5–25 Hz is obtained by the following formula:

$$Q_{\text{cn}} = r/c\kappa_v, \tag{8}$$

(see (2)), which with the assumed $c = 3.8$ km/s gives $Q_{cn} = 711$ (975) for this band. At the same time, for the frequency band near 1–2 Hz, Gusev and Shumilina (1999) and Abubakirov (2005) obtained the Q estimate for Eastern Kamchatka in the interval of 130–180. Hence, the presence of the frequency dependence of Q is undoubted. Assuming this dependence in the form $Q(f) = Q_0 f^{\gamma}$, one can easily derive the relationships for converting the estimates of κ_v obtained on a given frequency interval $[f_2, f_1]$ into the quantity Q_0 at arbitrary γ:

$$Q_0 = \frac{r\left(f_2^{1-\gamma} - f_1^{1-\gamma}\right)}{c\kappa_{v12}(f_2 - f_1)}, \tag{9}$$

where

$$\kappa_{v12} = -\frac{\log_{10} A(f_2) - \log_{10} A(f_1)}{\pi(f_2 - f_1)\log_{10} e} - \kappa_0, \tag{10}$$

is the κ_v estimate based on formulas (2), (3), and (7) for the given f_1, f_2, and r assuming that $\gamma = 0$. When deriving formulas (9) and (10), we took into account the fact that, in accordance with (7), the unknown nuisance parameter $\log A_0(f)$ is constant and frequency-independent. Quite speculatively assuming $\gamma = 0.42$, we obtain from (9) and (10) that at $r = 100$ (200) km, the value $Q_{cn} = 711$ (975) corresponds to $Q_0 = 140$ (191). For compensating the systematic distortion of the obtained estimates towards the higher values noted above, in the further calculations, we used $Q_0 = 165$ (225) for $r = 100$ (200) km with the linear extrapolation for the other values of r, assuming $q = -0.36$. We note for clarity that the values of Q_{cn} and Q_0 for $r = 200$ km are the averages over the distance interval [0 200] km. The loss estimates within the distance interval [100 200] km will be different. The values of $Q(f|r = 100$ km) are specified in accordance with the assumed preliminary model 2013 (Fig. 3).

Based on the described attenuation model (formulas (2) and (3)) and preliminary estimates κ_0, q, γ, and Q_0 ($r = 100$), each observed spectrum was corrected with allowance for the individual distance r. The example of the resulting spectral shape $A_1(f)$, together with the initial spectrum $A(f)$, is presented in Figs. 2b and 2c. The corrected spectra were interactively fitted by the near-optimal piecewise-power-law (piecewise-linear in Fig. 2a) approximations. For this, a subhorizontal segment with a slope of at most ± 0.5 is selected in the log-log graph of the spectrum $A_1(f)$, and the positions of the corners specifying f_{c2} and, if possible, f_{c3} are picked. There are cases when the position of f_{c3} cannot be determined: (1) the acceleration spectrum remains flat up to 30 Hz or up the last point of the spectrum with a reasonably high signal-to-noise ratio; (2) only one or two points of the averaged spectrum fall right of the spectral corner, and the f_{c3} estimate is evidently unreliable. In these two cases, for estimating the attenuation, instead of f_{c3}, the actual upper boundary f_t was used as the upper limit of the approximately flat $A_1(f)$ spectrum. There were also "degenerate" cases: $f_{c1} \approx f_{c2}$, the spectrum obeys (6) and difficulties do not arise; $f_{c2} \approx f_{c3}$, the spectrum has a pronounced single peak instead of a plateau, and estimating the attenuation is impossible (although f_{c3} can be determined). We denote the limits of the working frequency band by $[f_1, f_2]$, where f_1 is f_{c2} or f_{c1} and f_2 is f_{c3} or f_t. In the cases when the working bandwidth $\Delta f = f_2 - f_1$ was larger than 2 Hz, the spectrum was treated as acceptable for estimating the attenuation. The selection by this criterion among the initial 438 spectra yielded $N = 384$ spectra, which were used in the further analysis.

ESTIMATING THE ATTENUATION PARAMETERS AND THE RESULTS

Calculation procedure. In the further analysis, the parameters κ_0, Q_0^{-1}, γ, and q were treated as unknown. For convenience, we redesignated these variables by x_i, $i = 1, 2, 3, 4$. The difference in $\log A$ at frequencies f_2 and f_1 was denoted by

$$y_j = \log A(f_2) - \log A(f_1), \tag{11}$$

where j is the number of a given observation, $j = 1, 2, \ldots N$. Each observed spectrum recorded at distance r_j gives the equation

$$y_j - F_j(x_i) = \varepsilon_j, \tag{12}$$

where, based on formulas (2), (3), and (4),

$$\begin{aligned} F_j(x_i) = &-\pi Q_0^{-1}\left(f_2^{1-\gamma} - f_1^{1-\gamma}\right) \\ &\times \left(1 + \frac{q(r_j - 100)}{100}\right)\frac{r_j}{c} - \pi\kappa_0\left(f_2 - f_1\right) \end{aligned} \tag{13}$$

and ε_j is the small residual error with a presumably zero mean. The resulting redundant system of N nonlinear equations (12) was solved by the Nelder–Mead simplex method by minimizing the weighted sum of the squared residuals. The method converges stably. We used two weight types: the unit weights and those equal to Δf. The obtained estimates of κ_0, Q_0^{-1}, γ, and q (or, in the compact form, $\hat{x}_i$) are presented in Table 1. The residuals as the function of a number of the

Table 1. The numerical estimates of attenuation parameters

	Parameter				
	κ_0, s	Q_0	γ	q	$0.43\sigma(\varepsilon)$[1]
2011[2]	0.016	140	0.42	–0.36	–
2013[3]	0.016	165	0.42	–0.36	–
W0[4]	0.027	140	0.542	–0.18	0.068
W1[5]	0.030 ± 0.0050	156 ± 33	0.55 ± 0.082	-0.13 ± 0.071	0.079

[1] weighted root mean square residual of fitting y_i, in the units $\log_{10}A = 0.43\log A$; [2] the attenuation model based on κ_0 estimates from (Gusev and Guseva, 2011); [3] the initial model of attenuation according to (Gusev and Guseva, 2013) used for correcting the spectra; [4] the results of the inversion, the case when the equations have unit weights; [5], the results of the inversion, the case when an equation has a weight Δf; these results are treated as final. Each estimate of the parameter is indicated together with its standard deviation s_{JKj} by the DDJK method (see the text).

parameters are illustrated in Fig. 4, which shows $\delta\log_{10}A = 0.43(y_j - F_j(\hat{x}_i))$. Among the two versions of the weighting of the equations, the option where the weights are proportional to the operating bandwidth Δf was found to be preferable. We selected this option despite the fact that its weighted root-mean-square residual is slightly larger, because the variations Δf from one equation to another were high (2 to 10 Hz) and introducing the weights was evidently reasonable. In order to demonstrate the fact that introducing the weights does not change the result drastically, we also show the variant with the equal weights.

For determining the accuracy of the obtained estimates, we applied the deleted-d jackknife (DDJK) method using 20 subsets of the initial set of Eqs. (11), each with a random removal of 10% of the volume of the initial set. The DDJK estimate $s_{JK,i}$, for the standard deviation of estimate x_i, is calculated as

$$s^2_{JK,i} = \frac{N-D}{D}\sum (x_{ik} - x_i(\cdot))^2 \Big/ L, \qquad (14)$$

$$x_i(\cdot) = \sum x_{ik}/L, \qquad (15)$$

where $k = 1, 2, ..., L$ is the number of the subset, $D = 38$ is the number of the rejected equations, and $x_i(\cdot)$ is the mean of the estimates x_{ik} over the individual subsets. The values of $s_{JK,i}$ and the confidence intervals based on them are presented in Table 1.

Discussion of the results of the inversion. Based on the data of Table 1, we compared the corrections for the attenuation which were actually applied for correcting the spectra by model "2013" with the similar corrections expected from the new variant W1. A comparison demonstrated the absence of any significant systematic discrepancies, the almost perfect agreement at $r = 100$ km, and certain moderate inconsistencies at $r = 200$ km. In principle, it is possible to repeat the correction of the observed spectra, to reestimate f_{c2} and f_{c3} values, and to redetermine the parameters of the attenuation. However, since the final model of losses turned out to be close to the initial one, further refinements were unnecessary.

The correctness of the inversion was controlled by analyzing the dependence of the inversion residuals on the following parameters: the hypocentral distance, the central frequency and upper cutoff of the operating bandwidth, and magnitude M_L. The results are illustrated in Fig. 4. The systematic trends and strong outliers are absent, which provides the grounds to believe that the estimates of the parameters yielded by the inversions are quite reliable. However, it should be noted that the accuracy of these estimates ($\pm 1\sigma$) is low: it is ~20% for Q_0 and 15% for γ. The estimate of γ significantly differs from zero; hence, the growth of Q with frequency can be treated as an established fact. The obtained estimates for q indicate the reality of the decrease in the losses (Q^{-1}) with distance, albeit, at a rather low significance level (~10%). The estimate of κ_0 is close to the upper limit of the common variations of this parameter for a hard-rock station. As a rule, these estimates lie in the interval 0.005–0.025 s with a typical value of 0.015 s. However, this discrepancy should not be given an overextended interpretation because the obtained estimate is mainly formal. As demonstrated by Fig. 4, the data at small hypocentral distances are almost absent and the estimate is, in fact, an extrapolation from the distance interval 80–220 km. Quite probably, the preliminary estimate $\kappa_0 = 0.016$ s is closer to the actual value, whereas the true dependence $Q(f)$ is somewhat more gradual. The span of the confidence intervals for Q_0 and γ allows significant deviations from the trend identified by the formal minimization.

Considering the described problem of estimating κ_0 for the PET station in the absence of sources at the hypocentral distances shorter than 80 km, we note that difficulties could arise even if such data were available. In particular, the estimate of κ_0 can contain a noticeable systematic error even for the stations installed at the hard-rock sites due to the unaccounted velocity profile. In (Boore, 2013) it is shown for the typical hard-rock conditions that the velocities in the upper-

most portions of the section can steeply and monotonically drop; as a result, such a column forms a consistent smooth growth of the transfer function of the medium in the frequency band of 5 to 15 Hz. This frequency-dependent enhancement of the amplitudes leads to the negative shift of the empirical estimate of κ_0 relative to its true value, which is purely determined by the losses. This was practically established for South Korea (Jo and Baag, 2007) when 7 of 15 studied hard-rock stations showed zero or negative κ_0 estimates. Thus, one should expect that the κ_0 estimates may well be distorted towards the lower values due to the transfer function of the uppermost portion of the section.

For the PET station, Pavlenko (2013) presented a detailed estimate of the transfer function for the column beneath the site. The estimate was derived on the basis of the presumed velocity profile constructed by averaging the seismic sounding data. Based on this transfer function in the frequency band of 5 to 30 Hz, it was possible to estimate the effective addition to κ_0, which was found to be −0.06 s. Considering the significant (about ±50%) scatter of the estimates of the velocity column which were used for calculating the transfer function, and the actual, not very high accuracy of κ_0 estimates in the present work, we disregarded this effect.

The analysis of the components of attenuation. It was interesting to obtain the estimates of the different types of losses for the vicinities of the PET station and to compare the estimates based on the different sources for Eastern Kamchatka. Table 2 compares the estimates of the attenuation parameters expressed in terms of the Q-factor for (1) total losses Q_t, (2) the losses due to the wide-angle scattering Q_{sc}, and (3) inelastic losses Q_i. These parameters are qualitatively different, and the linkage between them is described by the relationship $Q_t^{-1} = Q_{sc}^{-1} + Q_i^1$. The results of the interpretation of the records in the present study only refer to Q_t. The values of Q_{sc} are taken from the publications, and the Q_i estimates are calculated as $Q_i^1 = Q_t^{-1} - Q_{sc}^{-1}$. Row 1 in Table 2 presents the Q_t values derived in (Abubakirov, 2005) from the behavior of the calibration function for the Fedotov class K^{F68} for the S-waves (Fedotov, 1972). Row 2 contains the Q_t values corresponding to the extinction length $r_Q = 90$ km obtained from the macroseismic data in (Gusev and Shumilina, 1999). Both data types are not strongly frequency-specific; they characterize the losses in terms of the coefficient of attenuation:

$$\alpha = \frac{d \log A(f)}{dr} = \frac{\pi f}{cQ(f)} \qquad (16)$$

(the corollary of (2)). For using these important data, we ascribed them to the bandwidths centered at 3 and 1.5 Hz, respectively. Rows 3 and 4 cite the estimates Q_t from (Abubakirov, 2005), which were obtained in two ways: by solving the inverse problem based on the envelope shapes by the MLTWA method and by analyzing the decrease with distance of the S-wave spectra normalized to the coda. Among these two estimates, the last one appears to be more reliable. Row 5 presents the Q_t estimates determined in the present work from the spectral decay (row W1 in Table 1). There is a reasonably close agreement between the numbers in rows 4 and 5, which indicates the absence of contradictions between the estimates obtained by the two fundamentally different methods from close groups of the data.

The next rows present the Q_{sc} estimates. Rows 6 and 7 show the estimates derived from the rate of the S-wave group ("noise pulse") broadening with distance by two methods: those derived from the estimates for the subvertical rays according to (Gusev and Abubakirov, 1999) and the direct estimates for the subhorizontal rays according to (Petukhin and Gusev, 2003). Row 8 is the estimate obtained by Abubakirov (2005) by the MLTWA method and corrected by him in order to allow for the possible inadequacies of the model of the medium accepted within the MLTWA method.

The close agreement within the groups of the Q_t and Q_{sc} estimates is notable. Such close agreement is uncommon for this type of data. The presence of this agreement legitimates constructing the derivative estimates Q_i by the cited formula $Q_i^{-1} = Q_t^{-1} - Q_{sc}^{-1}$. Row 10 presents the estimates Q_i calculated in the described way from the data of rows 5 and 7. Row 11 also shows the albedo estimates of the medium, B, which yield the relative fraction of the scattering-related (elastic) losses compared to the total losses: $B = Q_{sc}^{-1} / Q_t^{-1}$. We also cite the smoothed frequency dependence for the parameter of inelastic losses Q_i: $Q_i = 470 f^{0.27}$.

Figure 5 illustrates the behavior of the parameters of the losses as a function of distance for a set of the frequency bands. This behavior is interesting to a certain extent, although the existing data are scarce and their quality is barely irreproachable. These data expand the information of Table 2 where the dependence on distance is absent. By examining Table 2 and Fig. 5, we note the following features. The inelastic losses are almost independent on distance. The losses due to scattering steeply drop with distance, whereas the total losses have an intermediate position. A qualitatively close picture is also observed for the dependence on frequency. The inelastic losses decrease with frequency although this decrease is slow; the losses due to scattering rapidly diminish with frequency, whereas the behavior of the total losses again falls between the inelastic and scattering-related losses. The relative contributions of scattering and inelasticity to the losses are described by the albedo parameter B. At $r = 100$ km, the scattering accounts for 70% losses at 1Hz to 30% at 25 Hz. The albedo slowly decreases with distance: the value of B at $r = 200$ km is lower by ~30%.

Table 2. The attenuation (Q-factor) parameters for Eastern Kamchatka

No.	Parameter[1]	Data type	r, km^2	Frequency, Hz						Data source
				1	1.5	3	6	12	24	
1	Q_t	Calibration function $K_{S1.2}^{F68}$	30–300			275				(Abubakirov, 2005)
2	Q_t	Macroseismic $I(M, r)$,	80–300		212					(Gusev and Shumilina, 1999)
3	Q_t	MLTWA,	80–160		145	245	355			(Abubakirov, 2005)
4	Q_t	$A(f)$ vs r	80–160	[170]	225	281	355			(Abubakirov, 2005)
5	Q_t	$A(f)$ vs f	100	156	195	287	422	621	913	This work
6	Q_{sc}	Broadening, vertical ray	[a]100		[297]	555	[1036]			(Gusev and Abubakirov, 1999)
7	Q_{sc}	Broadening, horizontal ray	100	[283]	328	519	980	2146	[5000]	(Petukhin and Gusev, 2003)
8	Q_{sc}	MLTWA, corrected	80–160			500	1000			(Abubakirov, 2005)
10	Q_i	Rows 5, 7	100	[450]	483	643	742	874	[1100]	This work
11	B^3	Rows 5, 7	100	[0.55]	0.60	0.55	0.43	0.29	[0.16]	This work

[1] Q_t, Q_{sc}, and Q_i stand for the Q-factor due to the total losses, scattering-related losses, and inelastic losses, respectively. The extrapolations with the different but always limited reliability are indicated in the brackets; [2] the interval of the distances or the distance corresponding to the cited estimates; [3] albedo.

Estimates of the source parameter f_{c3}. For the same set of the earthquake records as that studied in the present work, in our recent paper (Gusev and Guseva, (2014), we describe and discuss the estimates for the characteristic (corner) frequencies f_{c1}, f_{c2}, and f_{c3} (Fig. 1) of the source spectra. Here, we only briefly summarize these results. The source spectra of the studied earthquakes typically have several characteristic (corner) frequencies f_{c1}, f_{c2}, and f_{c3}, where the trend of the source displacement spectrum changes from f^0 to f^{-1}, from f^{-1} to f^{-2}, and from f^{-2} to f^{-3}, respectively. Although in a number of cases $f_{c1} \approx f_{c2}$, which agrees with the common spectral model ω^{-2}, most spectra have a more complicated character. For most of the studied earthquakes, the source acceleration spectra have an upper cutoff (i.e., frequency f_{c3} is observed). This is an important fact because the existence of f_{c3} (the source-controlled f_{max}) is renounced in the bulk of the seismological literature. A slow decrease of f_{c3} with magnitude M_L is reliably observed against the significant scatter of the values (Fig. 6). The sense of the trend (declining rather than growing or constant) is plausible from the physical standpoint; however, the numerical value $d\log_{10}f_{c3}/dM = -0.11 \pm 0.017$ is much smaller than expected in the case of the hypothesized similarity of the sources (−0.5) and realistic assumption $M_L \approx M_W$. The result is interesting per se; besides, it provides a certain additional argument in favor of the approach developed in the present work, which presumably enables the estimates of f_{c3} to be obtained on a routine (mass) basis.

DISCUSSION

A comparison of the attenuation parameters estimated in the present work for the vicinity of the PET station with the estimates obtained in the same region by the other methods is presented above in Table 2. The results of this comparison can be treated as quite reasonable. The agreement between the Q_t estimates in rows 4 and 5 of Table 2 is particularly important. These estimates are obtained from commensurate data sets by two qualitatively different methods: by the direct method (from amplitude attenuation) and by the spectral method. In the Introduction it was explained that in the calculations of the estimates by these methods, each one requires accepting its own set of important assumptions, which are barely verifiable and could be inaccurate. Considering this, the results obtained by each of these methods cannot be treated as final, and it is due to this that their agreement deserves attention.

It would be interesting to compare the changes in the loss parameters with distance for two regions. The graphs in Fig. 5 are superimposed by the curves $Q_t(r|f)$ for the western United States, which are obtained in (Trifunac, 1994) from the decay of the acceleration spectra for the frequency bands 5–9, 9–15, and 15–25 Hz. These curves are plotted (quite conventionally) on the graphs for the bands of 6, 12, and 25 Hz. As far as the presence of the decay in the losses with distance and the presence of the frequency dependence of Q_t are concerned, the results of (Trifunac, 1994) reasonably well agree with the cited estimates of $Q_t(r|f)$ for Kam-

chatka. The discrepancies in the absolute values of Q_t are significant; however, they fall within the common scatter of the Q estimates. Remarkably, Trifunac disregarded the probable influence of f_{c3} on the spectra; therefore, his estimates may well contain additional fictitious attenuation. This hypothesis is consistent with the sign of the differences.

The estimates of Q based on the data in the literature noticeably vary from one subduction zone to another. For example, for 3 Hz, according to Fig. 11 of (Rychert et al., 2008), the estimates fall in the interval 50–280, whereas our estimate is 287. Our estimate for γ quite closely agrees with the estimate for Alaska (0.4–0.5) (Stachnik et al., 2004). Oth et al. (2011) cite their own data and the data in the literature for Japan, which demonstrate a scatter of 0.4 to 0.7 in the γ estimates and from 50 to 250 in Q_0. Here, the probable dependence of the Q_0 estimate on distance is typically ignored.

However, in the case of a fixed processing technique, the scatter of the estimates is not very large. For example, by analyzing the tectonic tremor and the data for six segments of the different subduction zones, Yabe et al. (2014) obtained the attenuation estimates in the frequency band of 3–8 Hz, with the values of the parameter α in (16) differing from each other by at most a factor of two. In their study, these authors revealed clear indications of the Q estimates growing with the distance range used for obtaining these estimates. The authors of the cited work interpreted this as the result of a manifest decrease of the losses with depth. The Q estimates (for $f = 4.5$ Hz) for a distance interval of 50–150 km were 300–800 when derived from the tremor records and 300–400 when based on intraplate earthquake records. These values are commensurate with our estimates for $r = 100$ km which indicate that $Q \approx 350$ at $f = 4.5$ Hz.

It can be believed that the growing trend of Q_0 with distance accounts for a considerable part of the scatter in the published estimates: the low Q_0 estimates frequently refer to the hypocentral distances of at most 100 km or even up to 50 km. Generally, the scatter in the published estimates of Q and α is large both overall and for the subduction zones in particular (e.g., see the extensive review in (Yabe et al., 2014)). Moreover, it is quite clear that this scatter is largely contributed by the peculiarities of a particular technique used, which, however, does not exclude the scatter caused by the natural factors. Therefore, for gaining a full understanding, it is required to thoroughly investigate the particular discrepancies: between the sets of the a priori assumptions, between the methods for the measurements of the records and calculating the parameters, and between the ranges of the distances. A discussion of the differences between the regions or subregions only makes sense after excluding the differences associated with the cited factors. In particular, the obsolete results where Q was estimated from the decay of the peak amplitudes (with or without filtering) instead of the spectral amplitudes should be largely rejected from the analysis. Such a scrupulous analysis is barely relevant in the context of the present paper, which is not conceived as a review. At the same time, the cited examples still provide a certain view of the problem of the scatter in the Q estimates.

It would be interesting to compare the frequency trend of the losses due to the inelastic absorption with the laboratory data. There are estimates obtained in the laboratory conditions for the torsional oscillations of the polycrystalline olivine specimens for the frequencies of 0.01–1 Hz (Jackson et al., 2002). Of course, the assumption that the results obtained for polycrystalline olivine are applicable for the rock material on the S-wave paths studied by us is obviously crude; however, we accept it conditionally. The extrapolation to the frequency interval above 1Hz studied in our work is likely to be legitimate because the empirical trends are fairly close to linear. Then, the exponent of the power-law trend of inelastic losses revealed by our analysis (0.27) almost perfectly coincides with the laboratory estimate (0.26). Judging by the laboratory data, the losses Q_i^{-1} themselves could correspond to the temperatures of 800–900°C, which is much higher than the typical estimates (up to 600°C) for a seismically active lithosphere (McKenzie et al., 2005). The difference is significant and most likely to be due to the fact that the laboratory estimates are obtained in the dry synthetic specimens, whereas the lithosphere in the plate contact zone and nearby contains a considerable amount of the fluids which increase the inelastic losses. Stachnik et al. (2004) note the inconsistency between the frequency trend of the inelastic losses estimated in the laboratory experiments and the trend of the total losses Q_t^{-1} estimated from the seismological data. The present study shows that this disagreement is most likely to be apparent; it is also present in our data but disappears when we exclude the scattering-related losses from the seismological estimates and pass from Q_t^{-1} to Q_i^{-1}.

The obtained estimate $Q_i = 470f^{0.27}$ for the studied frequency band 1.5–25 Hz also fairly well agrees with the estimate $Q = 600f^{0.3}$ for the inelastic losses in the mantle overall in the interval 0.01–1 Hz according to (Lekić et al., 2009). Although these estimates refer to the nonoverlapping frequency bands, these bands are close to each other.

CONCLUSIONS

The original method for separating the contributions of the source and the medium into f_{max}, which is suggested and tested in the present work, for the first time provides a possibility to reveal systematic errors such as the overestimation of losses due to the neglect of the shapes of the source spectra and to exclude these errors from the attenuation estimates.

The obtained loss estimates and the revealed trends generally agree with the known patterns for the other regions. In particular, the frequency dependence of Q is quite typical. The decrease of the losses (Q^{-1}) with distance was also observed previously. The joint analysis of the influence of distance and frequency on the losses in the framework of a single inversion is probably interesting from the methodological standpoint. The close agreement revealed between the independent loss estimates for the same region by the spectral method (this work) and direct method (Abubakirov, 2005) is worth noting. Therefore, it can be believed that the obtained estimates are free of large distortions.

The fact that the frequency dependence of the inelastic losses estimated in the present work practically coincides with the similar estimates based on the laboratory data for polycrystalline olivine is particularly remarkable.

The large set of estimates obtained for the third corner frequency f_{c3}—the source spectrum parameter—is a by-pass product of our work from the standpoint of estimating the absorption; however, this is still an interesting result. Based on the extensive data, it was established that f_{c3} tends to decrease with magnitude. This trend, quite plausible from the physical standpoint, is interesting and important for the physics of the source of the earthquake.

ACKNOWLEDGMENTS

The work was carried out at the Kamchatka branch of the Geophysical Survey of the Russian Academy of Sciences with support from the Russian Science Foundation (project 14-17-00621).

REFERENCES

Abubakirov, I.R., Attenuation characteristics of transverse waves in the lithosphere of Kamchatka estimated from observations at the Petropavlovsk digital broadband station, *Izv., Phys. Solid Earth*, 2005, vol. 41, no. 10, pp. 813–824.

Anderson, J.G. and Hough, S.E., A model for the shape of the Fourier amplitude spectrum of acceleration at high frequencies, *Bull. Seismol. Soc. Am.*, 1984, vol. 74, pp. 1969–1993.

Boatwright, J., Fletcher, J.B., and Fumal, T.E., A general inversion scheme for source, site, and propagation characteristics using multiply recorded sets of moderate-sized earthquakes, *Bull. Seismol. Soc. Am.*, 1991, vol. 81, no. 5, pp. 1754–1782.

Boore, D.M., The uses and limitations of the square-root-impedance method for computing site amplification, *Bull. Seismol. Soc. Am.*, 2013, vol. 103, no. 4, pp. 2356–2368. doi 10.1785/01201202

Brune, J.N., Tectonic stress and the spectra of seismic shear waves from earthquakes, *J. Geophys. Res.*, 1970, vol. 75, pp. 4997–5009.

Castro, R.R., Massa, M., Augliera, P., and Pacor, F., Body-wave attenuation in the Region of Garda, Italy, *Pure Appl. Geophys.*, 2008, vol. 165, pp. 1351–1366. doi 10.1007/s00024-008-0365-1

Dainty, A.M., A scattering model to explain seismic Q observations in the lithosphere between 1 and 30 Hz, *Geophys. Rev. Lett.*, 1981, vol. 8, pp. 1126–1128.

Fedotov, S.A. and Boldyrev, S.A., On the frequency dependence of body-wave absorption in the crust and upper mantle of the Kuril Island Arc, *Izv. Akad. Nauk SSSR, Fiz. Zemli*, 1969, no. 9, pp. 17–33.

Fedotov, S.A., *Energeticheskaya klassifikatsiya kurilo-kamchatskikh zemletryasenii i problema magnitud* (Energy Classification of the Kuril–Kamchatka Earthquakes and the Problem of Magnitudes), Moscow: Nauka, 1972.

Fletcher, J.B. and Boatwright, J., Source parameters of Loma Prieta aftershocks and wave propagation characteristics along the San Francisco Peninsula from a joint inversion of digital seismograms, *Bull. Seismol. Soc. Am.*, 1991, vol. 81, p. 1783–1812.

Ford, S.R., Dreger, D.S., Mayeda, K., Walter, W.R., Malagnini, L., and Phillips, W.S., Regional attenuation in Northern California: a comparison of five 1D Q methods, *Bull. Seismol. Soc. Am.*, 2008, vol. 98, pp. 2033–2046. doi 10.1785/0120070218

Gordeev, E.I. and Rykunov, L.P., The spectra of R-waves from the remote earthquakes in the frequency band 1–10 Hz, *Izv. Akad. Nauk SSSR, Fiz. Zemli*, 1976, vol. 7, pp. 90–92.

Gusev, A.A., Descriptive statistical model of earthquake source radiation and its application to an estimation of short-period strong motion, *Geophys. J. R. Astron. Soc*, 1983, vol. 74, pp. 787–808.

Gusev, A.A., Descriptive statistical model of the earthquake source radiation and its application to estimating the short-period strong motion, *Vulkanol. Seismol.*, 1984, no. 1, pp. 3–22.

Gusev, A.A. and Abybakirov, I.R., Simulated envelopes of non-isotropically scattered body waves as compared to observed ones: another manifestation of fractal heterogeneity, *Geophys. J. Int.*, 1996, vol. 127, pp. 49–60.

Gusev, A.A., Gordeev, E.I., Guseva, E.M., Petukhin, A.G., and Chebrov, V.M., A first version of the $A_{max}(M_W,R)$ relation for kamchatka, *Pure Appl. Geophys.*, 1997, vol. 149, pp. 299–312.

Gusev, A.A., Guseva, E.M., Petukhin, A.G., Gordeev, E.I., and Chebrov, V.N. Peak ground accelerations in the Kamchatka Peninsula from data of strong motion instruments, *Izv., Phys. Solid Earth*, 1998, vol. 34, no. 4, pp. 283–290.

Gusev, A.A. and Abubakirov, I.R., Vertical profile of effective turbidity reconstructed from broadening of incoherent body-wave pulses: II. Application to Kamchatka data, *Geophys. J. Int.,* 1999, vol. 136, pp. 309–323.

Gusev, A.A. and Shumilina, L.S., Modeling the intensity–magnitude–distance relationship based on the concept of an incoherent elongated source, *Vulkanol. Seismol.*, 1999, nos. 4–5, pp. 29–40.

Gusev, A.A. and Guseva, E.M., Testing the applicability of the attenuation parameter kappa for a prompt and coarse estimation of the hypocentral distance: case study from the Petropavlovsk station data, in *Seismologicheskie i geofizicheskie issledovaniya na Kamchatke. K 50-letiyu detal'nykh seismologicheskikh nablyudenii* (Seismological and Geophysical Studies in Kamchatka: to the 50th Anniversary of Detailed Seismological Observations), Gordeev, E.I. and

Chebrov, V.N., Eds., Petropavlovsk-Kamchatskii: Novaya kniga, 2012, chap. 15, pp. 397–411.

Gusev, A.A., High-frequency radiation from an earthquake fault: a review and a hypothesis of fractal rupture front geometry, *Pure Appl. Geophys.*, 2013, vol. 170, pp. 65–93. doi 10.1007/s00024-012-0455-y

Gusev, A.A. and Guseva, E.M., Preliminary results on retrieving the characteristic frequencies in the source spectra of local earthquakes from the records by the Petropavlovsk-Kamchatskii station, in *Problemy kompleksnogo geofizicheskogo monitoringa Dal'nego Vostoka Rossii* (Problems of Complex Geophysical Monitoring in the Russian Far East), Petropavlovsk-Kamchatskii: Kamchatskii filial Geofizicheskoi sluzhby RAN, 2013, pp. 147–151.

Gusev, A.A. and Guseva, E.M., Scaling properties of corner frequencies of Kamchatka earthquakes, *Dokl., Earth Sci.*, 2014, vol. 458, no. 1, pp. 1112–1115.

Guseva, E.M., Gusev, A.A., and Oskorbin, L.S., The program package for numerical processing of seismic records and its testing by the example of some strong motion data, *Vulkanol. Seismol.*, 1989, no. 5, pp. 35–49.

Hanks, T.C., f_{max}, *Bull. Seismol. Soc. Am.*, 1982, vol. 72, pp. 1867–1879.

Hough, S.E., Anderson, J.G., Brune, J., Vernon, F., Berger, J., Fletcher, J., Haar, L., Hanks, T., and Baker, L., Attenuation near Anza, California, *Bull. Seismol. Soc. Am.*, 1988, vol. 78, pp. 672–691.

Jackson, I., Fitz Gerald, J.D., Faul U.H., and Tan, B.H., Grain-size sensitive seismic wave attenuation in polycrystalline olivine, *J. Geophys. Res.*, 2002, vol. 107, p. 2360. doi 10.1029/2001JB001225

Kinoshita, S., Local characteristics of the f_{max} of bedrock motion in the Tokyo metropolitan area, Japan, *J. Phys. Earth*, 1992, vol. 40, pp. 487–515.

Kurtulmus, T. and Akyol, N., Crustal attenuation characteristics in western Turkey, *Geophys. J. Int.*, 2013, vol. 195, pp. 1384–1394. doi 10.1093/gji/ggt318

Lekić, V., Matas, J., Panning, M., and Romanowicz, B., Measurement and implications of frequency dependence of attenuation, *Earth Planet. Sci. Lett.*, 2009, vol. 282, pp. 285–293.

Malagnini, L., Mayeda, K., Uhrhammer, R., Akinci, A., and Herrmann, R.B., A regional ground-motion excitation/attenuation model for the San Francisco Region, *Bull. Seismol. Soc. Am.*, 2007, vol. 97, pp. 843–862. doi 10.1785/0120060101E

McKenzie, D., Jackson, J., and Priestley, R., Thermal structure of oceanic and continental lithosphere, *Earth Planet. Sci. Lett.,* 2005, vol. 233, pp. 337–349.

Papageorgiou, A.S. and Aki, K., A specific barrier model for the quantitative description of inhomogeneous faulting and the prediction of the strong ground motion: I. Description of the model, *Bull. Seismol. Soc. Am.*, 1983, vol. 73, pp. 693–722.

Pavlenko, O.V., Simulation of ground motion from strong earthquakes of Kamchatka region (1992–1993) at rock and soil sites, *Pure Appl. Geophys.*, 2013, vol. 170, pp. 571–595.

Petukhin, A.G. and Gusev, A.A., The duration-distance relationship and average envelope shapes of small Kamchatka earthquakes, *Pure Appl. Geophys.*, 2003, vol. 160, pp. 1717–1743.

Purvance, M.D. and Anderson, J.G., A comprehensive study of the observed spectral decay in strong-motion accelerations recorded in Guerrero, Mexico, *Bull. Seismol. Soc. Am.*, 2003, vol. 93, pp. 600–611. doi 10.1785/0120020065

Rychert, C.A., Fischer, K.M., Abers, G.A., Plank, T., Syracuse, E., Protti, J.M., Gonzalez, V., and Strauch, W., Strong along-arc variations in attenuation in the mantle wedge beneath Costa Rica and Nicaragua, *Geochem. Geophys. Geosyst.*, 2008, vol. 9, Q10SD10. doi 10.1029/2008GC002040

Sasatani, T., Source characteristics of the 1994 Hokkaido Toho-oki earthquake deduced from wide band strong-motion records, *J. Fac. Sci. Hokkaido Univ., Ser. VII (Geophys.)*, 1997, vol. 10, pp. 269–293.

Stachnik, J.C., Abers, G.A., and Christensen, D.H., Seismic attenuation and mantle wedge temperatures in the Alaska subduction zone, *J. Geophys. Res.*, 2004, vol. 109, p. 10304. doi 10.1029/2004JB0032018

Trifunac, M.D., *Q* and high-frequency strong motion spectra, *Soil Dyn. Earthq. Eng.,* 1994, vol. 13, no. 3, pp. 149–161.

Tsai, Ch.-Ch.P. and Chen, K.-Ch., A model for the high-cut process of strong-motion accelerations in terms of distance, magnitude, and site condition: an example from the SMART 1 array, Lotung, Taiwan, *Bull. Seismol. Soc. Am.*, 2000, vol. 90, pp. 1535–1542.

Venkataraman, A., Rivera, L., and Kanamori, H., Radiated energy from the 16 October 1999 Hector Mine earthquake: regional and teleseismic estimates, *Bull. Seismol. Soc. Am.*, 2002, vol. 92, no. 4, pp. 1256–1265.

Wu, C.F.J., On the asymptotic properties of the jackknife histogram, *Ann. Stat.*, 1990, vol. 18, pp. 1438–1452.

Yabe, S., Baltay, A.S., Ide, S., and Beroza, G.C., Seismic-wave attenuation determined from tectonic tremor in multiple subduction zones, *Bull. Seismol. Soc. Am.*, 2014, vol. 104, pp. 2043–2059.

Ye, L., Lay, T., and Kanamori, H., Ground shaking and seismic source spectra for large earthquakes around the megathrust fault offshore of Northeastern Honshu, Japan, *Bull. Seismol. Soc. Am.*, 2013, vol. 103, pp. 1221–1241. doi 10.1785/0120120115

Translated by M. Nazarenko